Astron. Astrophys. 352, 355–362 (1999)

ASTRONOMY AND ASTROPHYSICS

Weak weak lensing: correcting weak shear measurements accurately for PSF anisotropy

Konrad Kuijken⋆

Kapteyn Astronomical Institute, P.O. Box 800, 9700 AV Groningen, The Netherlands (kuijken@astro.rug.nl)

Received 17 August 1999 / Accepted 5 October 1999

Abstract. We have developed a new technique for weak lensing analysis, specifically designed to correct accurately for the effect of the point spread function (PSF) on the shapes of small galaxy images. This method does not rely on weighted second moments of detected images, which we show can leave residuals at the level of a percent in the shear; rather, we directly fit observed galaxy images as PSF-convolved, sheared circular sources. We show by means of simulations that this technique is able to recover shears with systematic errors well below the percent level for representative PSF shapes, while its noise properties are similar to existing methods.

Key words: methods: data analysis – cosmology: gravitational lensing

1. Introduction

Gravitational lensing is one of the most powerful and direct methods for studying the gravitational potentials of massive objects in the universe. An important type of lensing study is 'weak lensing.' It is the study of mild systematic distortions of background sources as their light rays are perturbed by gravitational fields on their way to us. Weak lensing has already provided important results in the study of galaxy clusters (e.g., Tyson et al. 1990; Bonnet et al. 1993; Fahlman et al. 1994; Squires et al. 1997; Fischer et al. 1997; Clowe et al. 1998; Hoekstra et al. 1998), halos of individual galaxies (e.g., Brainerd et al. 1996), and large-scale structure (Schneider et al. 1998). As the techniques are becoming better understood, research is progressing to the search for weaker and weaker distortions, which would enable the outer regions of galaxy clusters and galaxy halos, as well as lensing signals from large-scale structure (e.g., Jain & Seljak 1997; Kaiser 1998), to be studied.

To be able to detect such very weak signals, it is important to accurately remove the dominant systematic effect affecting weak lensing measurements: anisotropy of, and smearing by, the point-spread function (PSF). In this paper we will first investigate the limits of the most commonly-used technique for weak lensing analysis, devised by Kaiser et al. (1995, henceforth KSB). We will show that after PSF anisotropy correction, residual effects on the order of 1% shear are difficult to avoid with this method, even for moderately elongated PSF's. Since the ability to detect percent signals is important for a variety of scientific questions, we have therefore devised a new method which does not have such residuals, but which nevertheless has noise properties comparable to those of the KSB method.

There are several other methods for PSF anisotropy correction in the literature. The Autocorrelation Function method of Van Waerbeke et al. (1997) is a variant of the KSB method in which not individual galaxy images, but the autocorrelation function of many of them, is analyzed. The Bonnet & Mellier (1995) method uses a different aperture weighting function from KSB, and treats the PSF convolution as a shear term. Fischer & Tyson (1997) convolve the image with a kernel constructed to make the PSF rounder again. A more sophisticated such kernel has recently been presented by Kaiser (in preparation).

2. Limitations of the KSB formalism for PSF anisotropy correction

We first examine the KSB method, following our earlier tests in the context of analysis of Hubble Space Telescope images (Hoekstra et al. 1998, Appendix D).

2.1. The KSB method

The technique of weak (or statistical) lensing involves measuring the systematic, gravitationally induced, distortion of background images behind a gravitational lens. In the weak lensing regime small background images are distorted by a shear (γ_1, γ_2) and a convergence κ, whose combined effect is represented by the mapping

$$\begin{pmatrix} x \\ y \end{pmatrix} \rightarrow \begin{pmatrix} 1-\kappa-\gamma_1 & -\gamma_2 \\ -\gamma_2 & 1-\kappa+\gamma_1 \end{pmatrix} \begin{pmatrix} x \\ y \end{pmatrix} \equiv (1-\kappa) \begin{pmatrix} 1-g_1 & -g_2 \\ -g_2 & 1+g_1 \end{pmatrix} \begin{pmatrix} x \\ y \end{pmatrix} \quad (1)$$

where $g_i = \gamma_i/(1-\kappa)$. For simplicity, in what follows we neglect κ as it is small in the weak lensing regime, and pretend we are deriving the true shear γ instead of the reduced shear g. Thus, our results on shape measurements are valid, but their

⋆ Visiting scientist, Department of Theoretical Physics, University of the Basque Country

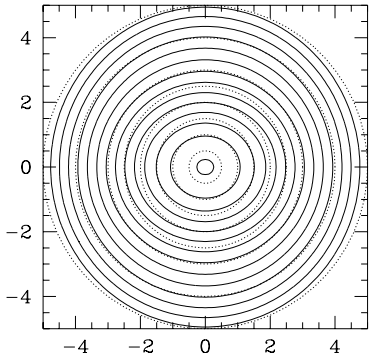

Fig. 1. An example of a PSF with radially varying ellipticity, but zero overall polarization. (Eq. (4) with $\delta = 0.3$). Contours differ by a factor of $2^{1/2}$. The dotted curves are circles, shown for comparison.

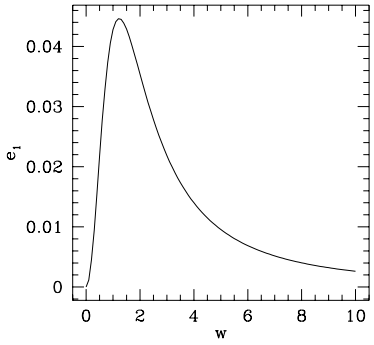

Fig. 2. The polarization of the PSF of Fig. 1 as a function of the weight function's Gaussian radius w. The plot shows that with compact weight functions such as those that are required to suppress photon noise, even mildly elongated PSF's may erroneously yield a polarization of several percent.

interpretation as a lensing signal may require consideration of the $(1-\kappa)$ factor. Our analysis makes no assumptions on the smallness of g_i, though.

KSB describe a method for recovering (γ_1, γ_2) from images of distant galaxies. Essentially, they derive galaxy ellipticities from weighted second moments of the observed images, and then correct these for the effects of the weight function and of smearing by the point spread function (PSF). By averaging over many galaxies, which are assumed to be intrinsically randomly oriented, the effect of individual galaxy ellipticities should average out, leaving the systematic lensing signal. The KSB method has proved to be very effective, especially in the study of galaxy cluster potentials.

KSB define various "polarizabilities", which express the ratio between an input distortion (gravitational shear or PSF anisotropy) and the measured polarization

$$e = \left(\frac{I^w_{xx} - I^w_{yy}}{I^w_{xx} + I^w_{yy}}, \frac{2I^w_{xy}}{I^w_{xx} + I^w_{yy}} \right) \tag{2}$$

of an image $f(x,y)$. These polarizations are derived from weighted second moments

$$I^w_{xx} = \int f(x,y) x^2 W(r) dxdy, \qquad \text{etc.,} \tag{3}$$

of the image intensities, where W is a weight function which goes to zero at large radii. The weight function is required as otherwise the sky noise in the outer parts of the image dominates the measured moment. The significance of the measurement is optimized by taking the weight function to be relatively compact, of a size comparable to the image itself.

Details of the method can be found in KSB, and in Hoekstra et al. (1998, henceforth HFKS), where a few small errors in the formulae of KSB were corrected. For the purposes of the present paper, it is sufficient to know that in the KSB formalism, the "smear polarizability" $P^{\rm sm}$ defines the ratio between the PSF anisotropy $p = (I_{xx} - I_{yy}, 2I_{xy})$, constructed from the unweighted second moments I_{ij} of the (normalized) PSF, and the resulting change in image polarization e. The "shear polarizability" $P^{\rm sh}$ is the ratio between the applied shear (γ_1, γ_2) and the resulting change in the image polarization. KSB show how the polarizabilities can be derived from higher weighted moments of the observed PSF and galaxy images.

2.2. How accurate is KSB?

In the context of ground-based cluster weak lensing, the KSB method works well. Nevertheless, it does involve some approximations. Now that weaker and weaker signals are of interest, it is therefore important to understand the limitations of the method. As already discussed by HFKS, for strongly non-Gaussian PSF's the KSB method does not completely correct PSF anisotropy. This is particularly true when analyzing small galaxies in deep HST images, where it turns out that the choice of weight function in Eq. (3) is important.

A simple PSF model can be used to illustrate why such residuals are, at some level, unavoidable. Consider the following PSF:

$$P(x,y) = G(1+\delta, 1) + G(4-\delta, 4), \tag{4}$$

where $G(a^2, b^2)$ is a unit-integral Gaussian of x- and y-dispersions a and b. δ is a small parameter. The case $\delta = 0.3$ is plotted in Fig. 1.

The PSF of Eq. (4) has exactly zero anisotropy p: the second moments in x and in y are equal. However, the ellipticity of the PSF varies with radius, which means that the *weighted* second moments are not equal: weighting the central parts more will enhance the x-moment preferentially. In fact, it is easy to show that the polarization constructed with weighted moments is $O(\delta)$. The precise result for a Gaussian weight function $W = \exp(-\frac{1}{2} r^2/w^2)$ is

$$e_1 = \frac{9\,w^2\,\left(7 + 5\,w^2 + w^4\right)\,\delta}{2\,\left(1+w^2\right)\,\left(4+w^2\right)\,\left(20 + 16\,w^2 + 5\,w^4\right)} + \mathrm{O}(\delta^2). \tag{5}$$

The polarization of the $\delta = 0.3$ PSF plotted in Fig. 1 is plotted in Fig. 2. It has a value of 0.03 near $w = 2$, roughly the radius of maximum significance which should be used to minimize photon noise in the polarization measurement.

The KSB polarizabilities are derived assuming that the PSF can be written as the convolution of a *compact* anisotropic part

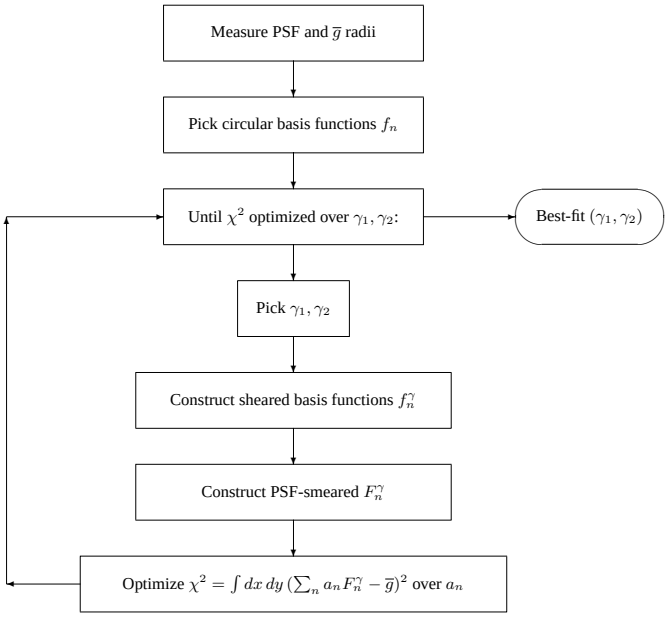

Fig. 3. The schematic algorithm used to derive the shear from an observed mean galaxy and PSF image.

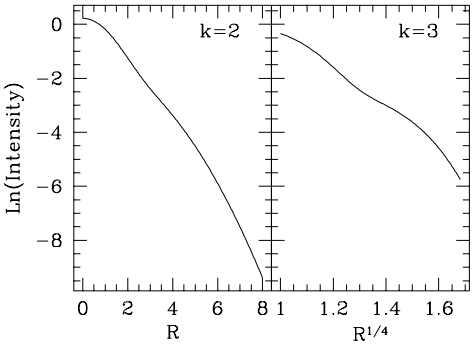

Fig. 4. The radial profiles of the double-Gaussian models used in this paper. Left, the $k = 2$ profile is plotted logarithmically to show its similarity to an exponential profile; right the $k = 3$ profile is plotted logarithmically vs. $R^{1/4}$ to show it is similar to a de Vaucouleurs model.

with an *extended* circular part (KSB Eq. A1). This assumption allows the anisotropy to be characterized in terms of p only. However, our example shows that this assumption may be too restrictive: it effectively couples the radial intensity profile of the PSF with its ellipticity profile. For example, a single Gaussian with constant ellipticity can be written as such a convolution, but a sum of two elliptical Gaussian such as the PSF of Eq. (4) cannot. The systematic errors that arise are the result of this.

3. A new method

Here we present a new method, with which the PSF effects can be corrected for with greater accuracy. The essence of the method is not to work with the moments of the observed images; instead each image is fit directly as a PSF-convolved, sheared circular source of unknown radial profile.

Assume for the moment that we have managed to sum the images of many galaxies into an 'average galaxy' image $\overline{g}(x, y)$. Analysing a stacked galaxy image is similar to the approach discussed by Lombardi & Bertin (1998), who average image second moments before corrections are applied. It differs from methods such as KSB or Bonnet & Mellier (1995) in which galaxies are individually corrected for PSF effects before they are combined to produce a shear estimate.

Intrinsically, $\overline{g}$ is circular if the galaxies are randomly oriented, but the image we observe has been distorted first by gravitational lensing shear, then by the atmospheric seeing, and finally by the camera optics. The observed $\overline{g}$ is therefore a sheared circular source, convolved with a (known) PSF. We fit $\overline{g}$ directly to such a model, with the minimum of further assumptions: in particular, the radial profile of $\overline{g}$ is left free. Note that the ellipticity of a sheared circular image is constant with radius, so after convolution with the PSF only a subset of ellipticity profiles is consistent with a shear.

If the PSF is known, e.g., from analysis of star images in the field, the model for $\overline{g}$ is specified by an unknown radial brightness profile, and by the shear parameters (γ_1, γ_2) that we are interested in. We model the radial profile as the superposition of several Gaussians of different fixed widths, and unknown amplitude. We have found that the following recipe for assigning the basis functions gives good results: (i) determine the best-fit circular Gaussian radii to the observed PSF and galaxy images, $r_{\rm PSF}$ and $r_{\rm GAL}$. (ii) Take $r = (r^2_{\rm GAL} - r^2_{\rm PSF})^{1/2}$ as an estimate for the intrinsic radius of $\overline{g}$. (iii) Use four components to describe the radial profile of $\overline{g}$, with Gaussian radii $(0.5, 1, 2, 4) \times r$.

The algorithm is laid out in Fig. 3. Tests of its accuracy and its sensitivity to noise in the images are described next.

3.1. Simulations in the absence of noise

As our first test, we considered simulated images of intrinsically round sources (no shear) observed with PSF's of a range of shape and anisotropy. A weak lensing analysis with an accurate correction for the PSF should yield zero shear. On a large number of model images, described below, we compared the results of the algorithm of Fig. 3 with those from the KSB algorithm as described in HFKS (implying in particular that the same weight function is used in the derivation of polarizations and polarizabilities of galaxy and PSF images). KSB polarizations are converted to shear estimates by dividing by the "pre-seeing shear polarizability" P^γ, for which we use the expression given by Luppino & Kaiser (1997). Unless stated otherwise, in all our simulations KSB was implemented with a weight function given by the best-fit circular Gaussian to the post-seeing galaxy image.

3.1.1. Double-Gaussian images and PSF

In most of our simulations, we modeled the sources and PSF as double gaussians

$$G\left[\sigma, (1-\epsilon_1)\sigma\right] + G\left[k\sigma, (1-\epsilon_2)k\sigma\right], \qquad (6)$$

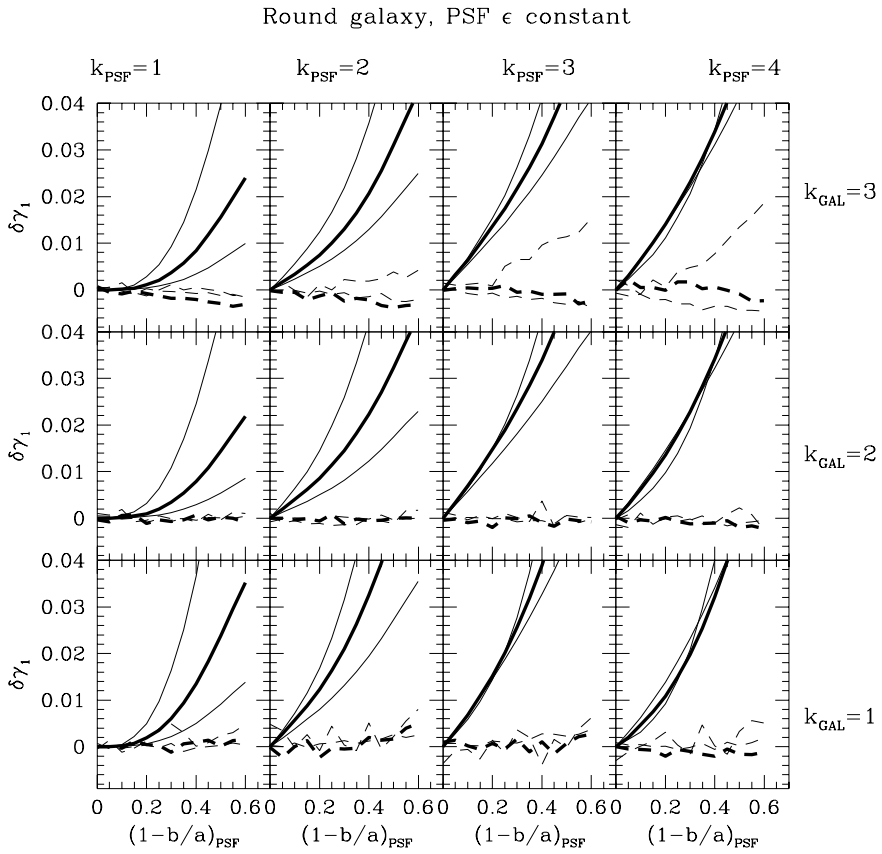

Fig. 5. The result of correcting simulated unsheared images for PSF anisotropy, following the KSB method (solid lines) and the method presented here (dashed lines). $\delta\gamma_1$ is in each case the shear that is deduced after the PSF correction, and should be zero for a perfect analysis. The k's are luminosity profile shape parameters for galaxy and PSF, and are explained in the text. In each panel the heavy line represents the case where the inner gaussian in the galaxy image is intrinsically of the same radius as the inner gaussian in the PSF (both have the same value of σ in Eq. (6)), the lighter lines those where the galaxy is 0.5 (upper) and 1.5 (lower) times this size. The PSF ellipticity is constant with radius in these simulations, with axis ratio $b/a = 1 - \epsilon$. While for the $k_{\rm PSF} = 1$ case (Gaussian PSF) the KSB method leaves a residual which is third-order in PSF ellipticity, other PSF luminosity profiles give rise to first-order residuals. The residuals of the new method in the upper panels disappear if more radial components are used in the fit for $\overline{g}$, highlighting that the dominant source of error in this method is the extent to which the radial profile is modeled correctly.

where $G[a,b] = \exp(-\frac{1}{2}x^2/a^2 - \frac{1}{2}y^2/b^2)/(2\pi ab)$. The parameter k is unity for a Gaussian profile, and is larger for more radially extended profiles. A reasonable, though admittedly crude, approximation to an exponential profile is given by setting $k = 2$, while $k = 3$ gives a reasonable approximation to a de Vaucouleurs profile (Fig. 4).

The ϵ_i allow different radial variations of ellipticity to be prescribed. Before shearing, the average galaxy is intrinsically round, so we set the ϵ_i equal to zero when modelling $\overline{g}$. PSF shapes can be more complicated, and we considered three kinds of PSF ellipticity profile: $\epsilon_1 = \epsilon_2$ (constant ellipticity with radius), $\epsilon_1 = 0$ (radially increasing ellipticity for $k > 1$) and $\epsilon_2 = 0$ (radially decreasing ellipticity). These three possibilities, though by no means exhaustive, form a representative set of PSF's.

The results of the simulations are presented in Figs. 5, 6 and 7. They show that the KSB method can suffer from systematic residuals around the 0.01 shear level once the PSF ellipticity exceeds 0.2 or so, whereas this is not so for the new method developed here. The KSB residuals are most important for small galaxies, for PSF profiles with long tails, and for radially increasing PSF ellipticity. The effect is clearly driven by the PSF shape, not by the galaxy brightness profile.

Notice that in the constant-ellipticity case (Fig. 5), with a Gaussian PSF ($k_{\rm PSF} = 1$) the residuals left by the KSB method are high order in PSF ellipticity, but that for non-Gaussian PSF's a low-order residual dominates. (We have verified this result analytically using symbolic mathematics.) This is a consequence of the fact that only the single elliptical Gaussian PSF can be written as a convolution of a compact anisotropic function with a round extended one, as assumed in the KSB derivation. It is clearly important to test algorithms not only for single-Gaussian PSF's!

3.1.2. A WFPC-2 PSF

In order to test whether our results are specific to the double-Gaussian formulation of the PSF, a test was also performed with a model PSF for the WFPC-2 camera on the Hubble Space Telescope. The model was generated with the TinyTIM software package, provided on-line at STScI by J. Krist. An oversampled PSF was calculated for a position near the corner of CCD#4, and convolved with a Gaussian circular galaxy of FWHM 0.25arcsec. This 'galaxy' and the PSF (Fig. 8) were then binned to a resolution of half a WFPC-2 pixel to avoid under-resolving the PSF, and analyzed as above. The results are summarized in Table 1, and confirm the results obtained from the large number of double-Gaussian simulations described earlier.

3.2. Noise properties

3.2.1. Analytic estimate

The error on the estimated shear due to photon noise can be estimated as follows. Let the 1-σ error on each pixel of $\overline{g}$ be s (for simplicity we take this to be the same on every pixel,

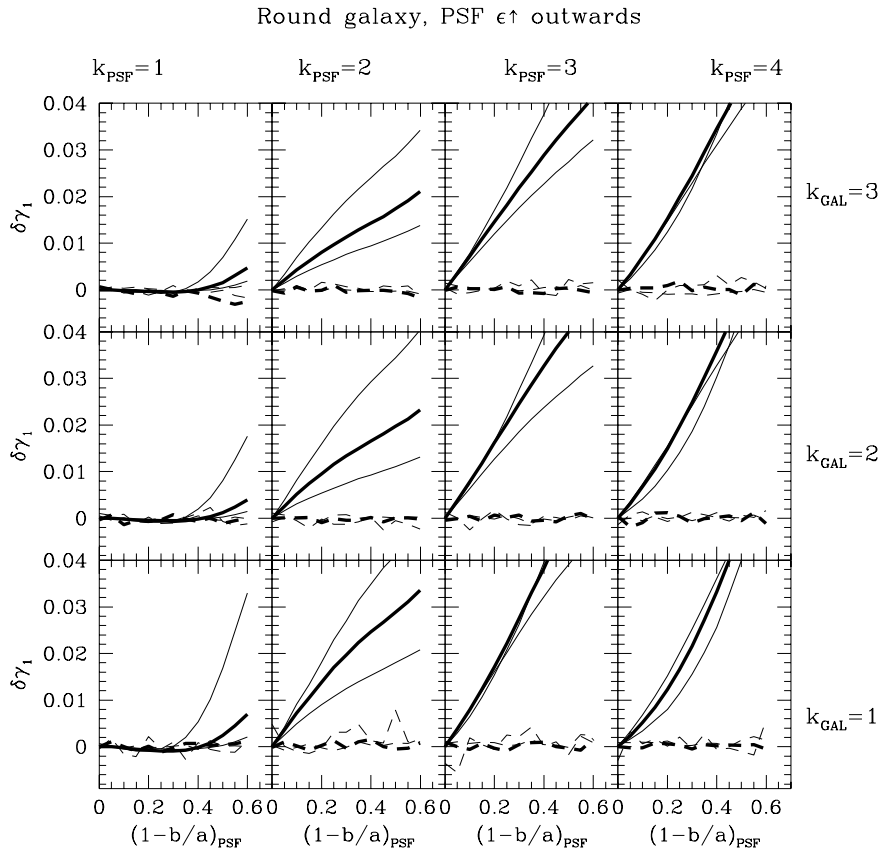

Fig. 6. As Fig. 5, but only the outer component of the PSF is elliptical, with axis ratio b/a.

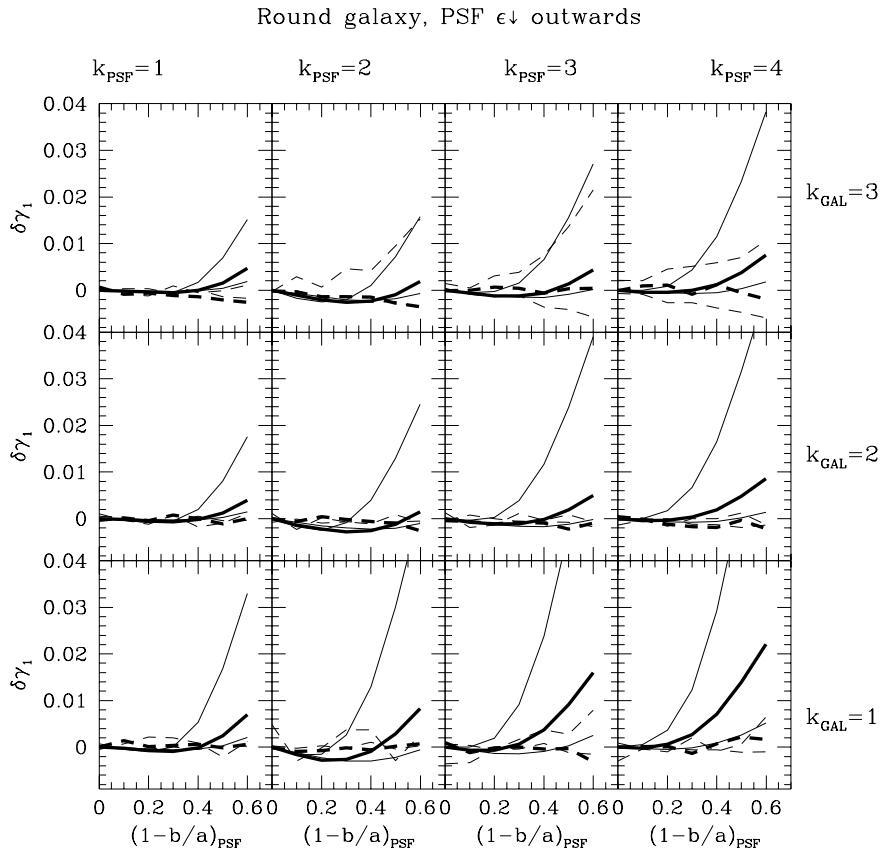

Fig. 7. As Fig. 5, but only the inner component of the PSF is elliptical, with axis ratio b/a.

Table 1. Results of a simulation based on a WFPC-2 PSF calculated using the TinyTIM software. In agreement with earlier results (HFKS), the KSB technique appears to over-correct for the anisotropic WFPC-2 PSF images slightly.

Weight function radius:	1.3 WFPC-2 pixels
PSF polarization:	$(-0.078, 0.024)$
Uncorrected galaxy e:	$(-0.020, -0.006)$
PSF-corrected galaxy γ:	$(-0.000, -0.019)$ (KSB)
	$(-0.000, -0.001)$ (new method)

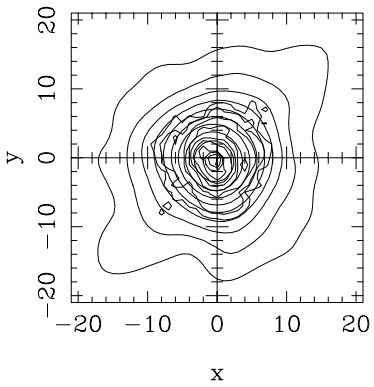

Fig. 8. PSF (jagged contours) and simulated galaxy image for an observation in the corner of one of the WFPC2 CCD's. Axis units are 0.05 arcsec.

appropriate for background-limited work). Then the shear is obtained by minimizing

$$\chi^2 = \sum_k \left[\overline{g}_k - (P \otimes f(\mathbf{x}\cdot\mathbf{\Gamma}^2\cdot\mathbf{x}))_k\right]^2 / s^2 \tag{7}$$

where $P(x,y)$ is the PSF, $f(r^2)$ is the intrinsic radial profile of the average galaxy, $\otimes$ denotes convolution, $\mathbf{x}_k$ is the position of the kth pixel, and $\mathbf{\Gamma}$ is the distortion matrix of Eq. (1). If the fit parameters γ_i are uncorrelated with the radial profile, their inverse variances are given by $\frac{1}{2}\partial^2\chi^2/\partial\gamma_i^2$. For example, at the best fit

$$\begin{aligned}\frac{1}{2}\frac{\partial^2\chi^2}{\partial\gamma_1^2} &= \sum_k \left(\frac{\partial}{\partial\gamma_1}(P\otimes f(\mathbf{x}\cdot\mathbf{\Gamma}^2\cdot\mathbf{x}))_k\right)^2 / s^2, \\ &= \sum_k \left(P\otimes[4f'(r^2)(y^2-x^2)]\right)^2 / s^2. \end{aligned}\tag{8}$$

The right-hand side of Eq. (8) can be estimated assuming that the PSF and observed average galaxy are Gaussians with dispersions $r_{\rm PSF}$ and $r_{\rm GAL}$ pixels of integral 1 and F, respectively. Then the 1-σ error on γ_1 evaluates to

$$\begin{aligned}\sigma(\gamma_1) &= \left(\frac{1}{2}\frac{\partial^2\chi^2}{\partial\gamma_1^2}\right)^{-1/2} = \frac{2\pi^{1/2}r_{\rm GAL}^3 s}{(r_{\rm GAL}^2 - r_{\rm PSF}^2)F} \\ &= \frac{r_{\rm GAL}^2}{(r_{\rm GAL}^2 - r_{\rm PSF}^2)}\frac{\delta F}{F}, \end{aligned}\tag{9}$$

where we have used the results that the PSF-fitting error on F for a Gaussian source is $\delta F = 2\pi^{1/2} r_{\rm GAL} s$. The error on γ_2 is the same. We have verified this formula by means of simulations, similar to those described below. Eq. (9) shows the expected increase in noise for small objects, as well as the lower limit, approached for fully resolved objects, of

$$\sigma(\gamma_i) \gtrsim \frac{\delta F}{F}. \tag{10}$$

3.2.2. Simulations with photon noise

We have checked the sensitivity to noise in the images by means of Monte Carlo simulation. Many realizations of random Gaussian noise superimposed on a PSF-smeared, intrinsically round galaxy image were analyzed with both algorithms, and the distributions of the resulting (γ_1, γ_2) estimates compared. Selected results are shown in Table 2. Interestingly, the effect of photon noise on the shear values derived with both methods is very similar, and there is once again no evidence for a bias in the results obtained with the new method.

A possible way to avoid the systematic residuals of the KSB method is to increase the radius of the weight function W in Eq. (3), since the problems arise from the imperfect way in which the polarizabilities represent the effect of W. However, the primary function of W is to control the noise in the images. Doubling the Gaussian radius of W does in fact improve the anisotropy correction in the mean, but at the cost of almost doubling the noise on the result (see Table 2).

3.2.3. The effect of centroiding errors

The centroid of an image can be determined in different ways, each of them susceptible to errors due to photon noise. The effect of centroiding errors on the summed galaxy image will be a convolution with the distribution of centroid errors. Thus, the PSF needs to be convolved with this distribution before analysis of $\overline{g}$, so that the effect of the centroiding error can be compensated.

4. Intrinsically elongated sources

In the method as described so far, the average galaxy $\overline{g}$ is analyzed. Very accurate shear measurements require $\overline{g}$ to be the average of a large number of galaxies (~ 1000 for a 1-σ shear accuracy of 0.01), otherwise intrinsic ellipticity scatter will dominate the measurement. However, constructing $\overline{g}$ is only possible if the shear and the PSF the same for all galaxies that are summed. Because of spatial variations of PSF and shear, this is usually not so.

We have therefore tested the algorithm in 'galaxy-by-galaxy' mode, fitting individual galaxies as PSF-smeared, intrinsically circular, sheared sources. The resulting shear estimates are then each dominated by the intrinsic galaxy shape, as

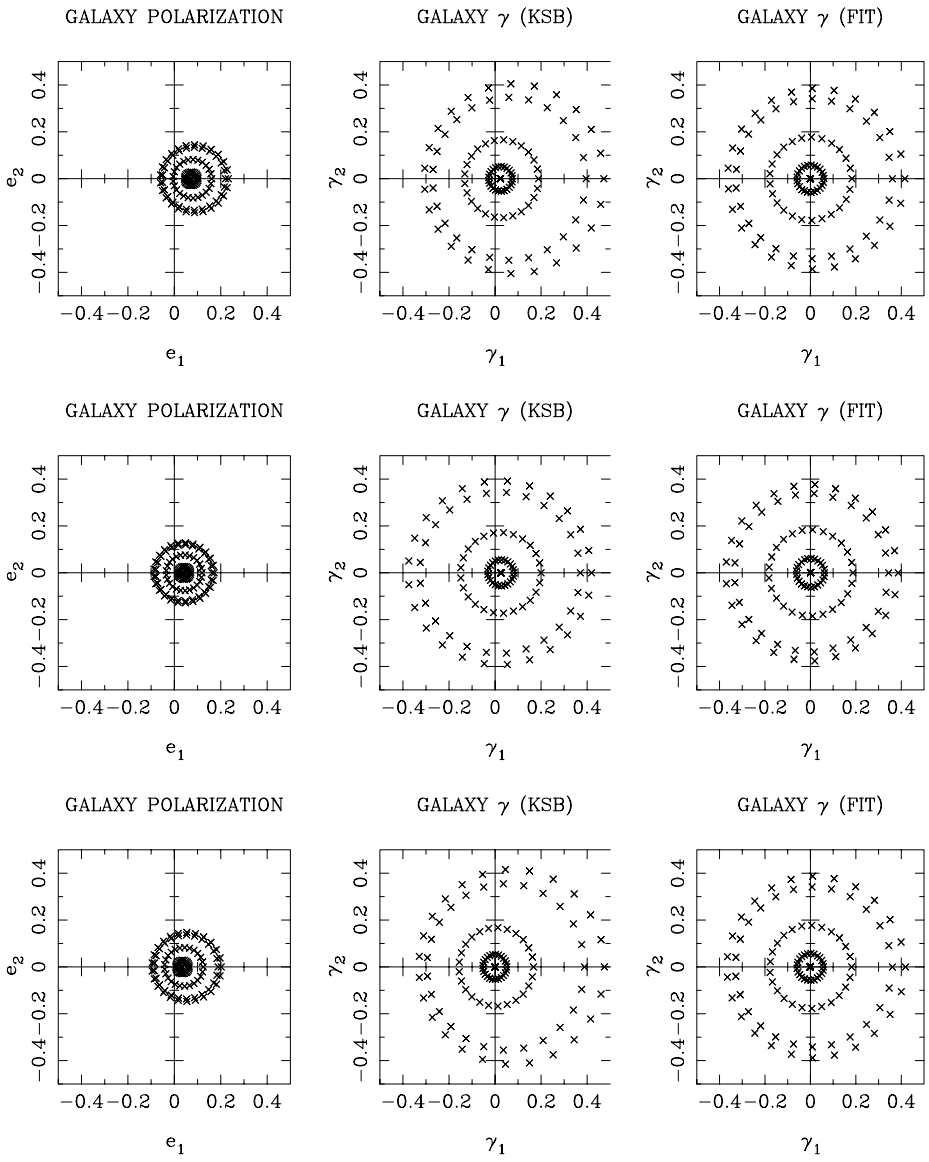

Fig. 9. The derived shear values from the algorithm applied to individual elongated 'disk+bulge' galaxy images, after smearing with an elongated PSF. Each ring of points represents a galaxy seen at many orientations; different rings correspond to different galaxy flattening. Left: the raw (e_1, e_2) polarizations measured with the standard KSB method, without correction for the PSF. Centre: the result of applying the KSB prescription for PSF anisotropy and circularization correction. The small bias seen before remains. Right: the result of the new algorithm on the same galaxies. In the latter case, the correct average shear estimate (zero) is recovered even though individual galaxies are not correctly described as intrinsically constant-ellipticity sources. The three rows refer to the three kinds of PSF ellipticity profile considered in Figs. 5–7: constant with radius (top), outward-increasing (middle), and outward-decreasing (bottom).

in KSB; the question is how well the average of such individually PSF-corrected shear estimates can represent the actual shear without bias. Note that galaxies are not generally well-described as constant-ellipticity sources, and hence there is no guarantee that, even in principle, the shear estimates will average to the correct value.

We ran our tests on various double-gaussian model galaxies, of differing axis ratios. To simulate typical galaxies, we included a round, central 'bulge' component, and an outer 'disk' of axis ratio between 0.1 and 1. (Simulations with different bulge axis ratios yielded essentially the same results.) These were placed at all orientations, smeared with various kinds of elliptical PSF, and analysed with the algorithm described above. The best-fit (γ_1, γ_2) values thus derived for each galaxy were then averaged to give an estimate of the shear.

As may be seen in Fig. 9, the new algorithm performs very well, essentially correcting all PSF anisotropy signal in the measured shear. By comparison, the slightly biased answer returned by the KSB algorithm is apparent as before. Residual systematics of the new method are at the level of a few tenths of a percent.

5. Summary

In this paper we have studied possible systematic errors arising from the correction for anisotropic point-spread functions in weak lensing analyses based on the well-known Kaiser et al. (1995) method. While such effects are small, generally below a few percent in the deduced gravitational shear components (γ_1, γ_2), they are at a level that is important for studies such as galaxy-galaxy lensing, lensing by large-scale structure or cluster lensing at large radii. We have traced the effect to the treatment in KSB of the PSF as a convolution of a compact anisotropic function with a more extended, circular function.

Table 2. Results from representative noise simulations of the KSB method and the one presented in this paper. In each case, 100 noise realizations (noise per pixel of 0.001, with (see Eq. (6) $\sigma_{\rm PSF} = 2$pixels, $k_{\rm GAL} = 2$ and total flux 4) were analyzed with the standard KSB method, with the KSB method using a weight function double the radius of the best-fit Gaussian, and with the new method described in this paper. The first six simulations were of cases without PSF anisotropy, and in the last six the PSF has a constant axis ratio of 0.7. In all cases, the dispersions of the standard KSB method and the new one are very similar, but note the imperfect correction from the KSB method. The simulations of KSB with a wider weight function show better correction for PSF anisotropy than the standard KSB implementation, but at the cost of increased noise.

KSB				This paper		
Standard W		Wider W		(4 radial cpts.)		
Mean	σ	Mean	σ	Mean	σ	Comments
0.0010	0.0084	0.0016	0.0142	0.0010	0.0079	Round Gaussian PSF, $\sigma_{\rm gal} = 0.5\sigma_{\rm PSF}$
0.0008	0.0067	0.0009	0.0105	0.0008	0.0061	Round Gaussian PSF, $\sigma_{\rm gal} = \sigma_{\rm PSF}$
0.0008	0.0072	0.0007	0.0113	0.0009	0.0066	Round Gaussian PSF, $\sigma_{\rm gal} = 1.5\sigma_{\rm PSF}$
0.0019	0.0149	0.0031	0.0310	0.0023	0.0150	Round $k = 3$ PSF, $\sigma_{\rm gal} = 0.5\sigma_{\rm PSF}$
0.0012	0.0104	0.0014	0.0206	0.0017	0.0110	Round $k = 3$ PSF, $\sigma_{\rm gal} = \sigma_{\rm PSF}$
0.0012	0.0105	0.0012	0.0186	0.0014	0.0107	Round $k = 3$ PSF, $\sigma_{\rm gal} = 1.5\sigma_{\rm PSF}$
0.0116	0.0056	0.0045	0.0097	0.0011	0.0061	$\epsilon = 0.3$ Gaussian PSF, $\sigma_{\rm gal} = 0.5\sigma_{\rm PSF}$
0.0041	0.0054	0.0017	0.0087	0.0009	0.0054	$\epsilon = 0.3$ Gaussian PSF, $\sigma_{\rm gal} = \sigma_{\rm PSF}$
0.0020	0.0064	0.0009	0.0102	0.0008	0.0060	$\epsilon = 0.3$ Gaussian PSF, $\sigma_{\rm gal} = 1.5\sigma_{\rm PSF}$
0.0277	0.0101	0.0222	0.0214	0.0023	0.0116	$\epsilon = 0.3$ $k = 3$ PSF, $\sigma_{\rm gal} = 0.5\sigma_{\rm PSF}$
0.0244	0.0085	0.0112	0.0162	0.0007	0.0091	$\epsilon = 0.3$ $k = 3$ PSF, $\sigma_{\rm gal} = \sigma_{\rm PSF}$
0.0191	0.0091	0.0061	0.0157	0.0008	0.0094	$\epsilon = 0.3$ $k = 3$ PSF, $\sigma_{\rm gal} = 1.5\sigma_{\rm PSF}$

We have presented a new algorithm with which to carry out the PSF-correction in a single fitting step. It makes no assumptions about the PSF other than that it is well-measured. We show with simulated images that the low-level residuals left in the KSB analysis can thus be avoided, and that the noise properties of this algorithm compare well with those of KSB.

The new algorithm is mathematically exact (in the sense that it will recover the correct shear value from a PSF-smeared image) when applied to instrinsically circular sources, provided the radial profile of the source can be modelled well. In the practical situation in which galaxies have intrinsic elongations but random orientations, we have shown that nearly unbiased results (down to a few tenths of a percent in shear) can also be obtained. This galaxy-by-galaxy application of the algorithm therefore allows observations with spatially varying PSF and/or shear fields to be handled.

Acknowledgements. I would like to thank Peter Schneider, Marijn Franx, Henk Hoekstra and the referee for critical readings of the manuscript and for suggesting several improvements.

References

Bonnet H., Mellier Y., 1995, A&A 303, 331
Bonnet H., Fort B., Kneib J.-P., Mellier Y., Soucail G., 1993, A&A 280, L7
Brainerd T., Blandford R.D., Smail I., 1996, ApJ 466, 623
Clowe D., Luppino G.A., Kaiser N., Henry J.P., Gioia I.M., 1998, ApJ 497, L61
Fahlman G., Kaiser N., Squires G., Woods D., 1994, ApJ 437, 56
Fischer P., Tyson J.A., 1997, AJ 114, 14
Fischer P., Bernstein G., Rhee G., Tyson J.A., 1997, AJ 113, 521
Hoekstra H., Franx M., Kuijken K., Squires G., 1998, ApJ 504, 636 (HFKS)
Jain B., Seljak U., 1997, ApJ 484, 560
Kaiser N., 1998, ApJ 498, 26
Kaiser N., Squires G., Broadhurst T., 1995, ApJ 449, 460 (KSB)
Lombardi M., Bertin G., 1998, A&A 330, 791
Luppino G.A., Kaiser N., 1997, ApJ 475, 20
Schneider P., Van Waerbeke L., Mellier Y., et al., 1998, A&A 333, 767
Squires G., Neumann D.M., Kaiser N., et al., 1997, ApJ 482, 648
Tyson J., Valdes F., Wenk R., 1990, ApJ 349, L1
Van Waerbeke L., Mellier Y., Schneider P., Fort B., Mathez G., 1997, A&A 317, 303